Comparing proton momentum distributions in A = 2 and 3 nuclei via 2H 3H and 3He (e, e′p) measurements

(Jefferson Lab Hall A Tritium Collaboration) Cruz-Torres, R.; Li, S.; Hauenstein, F.; Schmidt, A.; Nguyen, D.; Abrams, D.; Albataineh, H.; Alsalmi, S.; Androić, Darko; Aniol, K.; ...

Source / Izvornik: **Physics Letters B, 2019, 797**

Journal article, Published version
Rad u časopisu, Objavljena verzija rada (izdavačev PDF)

https://doi.org/10.1016/j.physletb.2019.134890

Permanent link / Trajna poveznica: https://urn.nsk.hr/urn:nbn:hr:217:399301

Physics Letters B 797 (2019) 134890

Contents lists available at ScienceDirect

Physics Letters B

www.elsevier.com/locate/physletb

Comparing proton momentum distributions in $A = 2$ and 3 nuclei via ^{2}H ^{3}H and ^{3}He $(e, e'p)$ measurements

Jefferson Lab Hall A Tritium Collaboration

R. Cruz-Torres [a], S. Li [b], F. Hauenstein [c], A. Schmidt [a], D. Nguyen [d], D. Abrams [d], H. Albataineh [e], S. Alsalmi [f], D. Androic [g], K. Aniol [h], W. Armstrong [i], J. Arrington [i], H. Atac [j], T. Averett [k], C. Ayerbe Gayoso [k], X. Bai [d], J. Bane [l], S. Barcus [k], A. Beck [a], V. Bellini [m], H. Bhatt [n], D. Bhetuwal [n], D. Biswas [o], D. Blyth [i], W. Boeglin [p], D. Bulumulla [c], A. Camsonne [q], J. Castellanos [p], J.-P. Chen [q], E.O. Cohen [r], S. Covrig [q], K. Craycraft [l], B. Dongwi [o], M. Duer [r], B. Duran [j], D. Dutta [n], E. Fuchey [s], C. Gal [d], T.N. Gautam [o], S. Gilad [a], K. Gnanvo [d], T. Gogami [t], J. Gomez [q], C. Gu [d], A. Habarakada [o], T. Hague [f], O. Hansen [q], M. Hattawy [i], O. Hen [a,*], D.W. Higinbotham [q], E. Hughes [u], C. Hyde [c], H. Ibrahim [v], S. Jian [d], S. Joosten [j], A. Karki [n], B. Karki [w], A.T. Katramatou [f], C. Keppel [q], M. Khachatryan [c], V. Khachatryan [x], A. Khanal [p], D. King [y], P. King [w], I. Korover [z], T. Kutz [x], N. Lashley-Colthirst [o], G. Laskaris [a], W. Li [aa], H. Liu [u], N. Liyanage [d], D. Lonardoni [ab,ac], R. Machleidt [ad], L.E. Marcucci [ae,af], P. Markowitz [p], R.E. McClellan [q], D. Meekins [q], S. Mey-Tal Beck [a], Z.-E. Meziani [j], R. Michaels [q], M. Mihovilovič [ag,ah,ai], V. Nelyubin [d], N. Nuruzzaman [o], M. Nycz [f], R. Obrecht [s], M. Olson [aj], L. Ou [a], V. Owen [k], B. Pandey [o], V. Pandey [ak], A. Papadopoulou [a], S. Park [x], M. Patsyuk [a], S. Paul [k], G.G. Petratos [f], E. Piasetzky [r], R. Pomatsalyuk [al], S. Premathilake [d], A.J.R. Puckett [s], V. Punjabi [am], R. Ransome [an], M.N.H. Rashad [c], P.E. Reimer [i], S. Riordan [i], J. Roche [w], F. Sammarruca [ad], N. Santiesteban [b], B. Sawatzky [q], E.P. Segarra [a], B. Schmookler [a], A. Shahinyan [ao], S. Širca [ag,ah], N. Sparveris [ap], T. Su [f], R. Suleiman [q], H. Szumila-Vance [q], A.S. Tadepalli [an], L. Tang [q], W. Tireman [aq], F. Tortorici [m], G. Urciuoli [ar], M. Viviani [af], L.B. Weinstein [c], B. Wojtsekhowski [q], S. Wood [q], Z.H. Ye [i], Z.Y. Ye [as], J. Zhang [x]

[a] *Massachusetts Institute of Technology, Cambridge, MA, USA*
[b] *University of New Hampshire, Durham, NH, USA*
[c] *Old Dominion University, Norfolk, VA, USA*
[d] *University of Virginia, Charlottesville, VA, USA*
[e] *Texas A & M University, Kingsville, TX, USA*
[f] *Kent State University, Kent, OH, USA*
[g] *University of Zagreb, Zagreb, Croatia*
[h] *California State University, Los Angeles, CA, USA*
[i] *Physics Division, Argonne National Laboratory, Lemont, IL, USA*
[j] *Temple University, Philadelphia, PA, USA*
[k] *The College of William and Mary, Williamsburg, VA, USA*
[l] *University of Tennessee, Knoxville, TN, USA*
[m] *INFN Sezione di Catania, Italy*
[n] *Mississippi State University, Miss. State, MS, USA*
[o] *Hampton University, Hampton, VA, USA*
[p] *Florida International University, Miami, FL, USA*
[q] *Jefferson Lab, Newport News, VA, USA*
[r] *School of Physics and Astronomy, Tel Aviv University, Tel Aviv 69978, Israel*

* Corresponding author.
E-mail address: hen@mit.edu (O. Hen).

https://doi.org/10.1016/j.physletb.2019.134890

[s] University of Connecticut, Storrs, CT, USA
[t] Tohoku University, Sendai, Japan
[u] Columbia University, New York, NY, USA
[v] Cairo University, Cairo, Egypt
[w] Ohio University, Athens, OH, USA
[x] Stony Brook University, State University of New York, NY, USA
[y] Syracuse University, Syracuse, NY, USA
[z] Nuclear Research Center -Negev, Beer-Sheva, Israel
[aa] University of Regina, Regina, SK, Canada
[ab] Facility for Rare Isotope Beams, Michigan State University, East Lansing, MI 48824, USA
[ac] Theoretical Division, Los Alamos National Laboratory, Los Alamos, NM 87545, USA
[ad] Department of Physics, University of Idaho, Moscow, ID 83844, USA
[ae] Department of Physics "E. Fermi", University of Pisa, Italy
[af] INFN, Pisa, Italy
[ag] University of Ljubljana, Ljubljana, Slovenia
[ah] Faculty of Mathematics and Physics, Jožef Stefan Institute, Ljubljana, Slovenia
[ai] Institut für Kernphysik, Johannes Gutenberg-Universität Mainz, DE-55128 Mainz, Germany
[aj] Saint Norbert College, De Pere, WI, USA
[ak] Center for Neutrino Physics, Virginia Tech, Blacksburg, VA 24061, USA
[al] Institute of Physics and Technology, Kharkov, Ukraine
[am] Norfolk State University, Norfolk, VA, USA
[an] Rutgers University, New Brunswick, NJ, USA
[ao] Yerevan Physics Institute, Yerevan, Armenia
[ap] Tel Aviv University, Tel Aviv, Israel
[aq] Northern Michigan University, Marquette, MI, USA
[ar] INFN, Rome, Italy
[as] University of Illinois-Chicago, IL, USA

ARTICLE INFO

Article history:
Received 11 June 2019
Received in revised form 14 August 2019
Accepted 21 August 2019
Available online 28 August 2019
Editor: D.F. Geesaman

ABSTRACT

We report the first measurement of the $(e, e'p)$ reaction cross-section ratios for Helium-3 (^{3}He), Tritium (^{3}H), and Deuterium (d). The measurement covered a missing momentum range of $40 \leq p_{miss} \leq 550$ MeV/c, at large momentum transfer ($\langle Q^2 \rangle \approx 1.9$ (GeV/c)^2) and $x_B > 1$, which minimized contributions from non quasi-elastic (QE) reaction mechanisms. The data is compared with plane-wave impulse approximation (PWIA) calculations using realistic spectral functions and momentum distributions. The measured and PWIA-calculated cross-section ratios for ^{3}He/d and ^{3}H/d extend to just above the typical nucleon Fermi-momentum ($k_F \approx 250$ MeV/c) and differ from each other by $\sim 20\%$, while for ^{3}He/^{3}H they agree within the measurement accuracy of about 3%. At momenta above k_F, the measured ^{3}He/^{3}H ratios differ from the calculation by $20\% - 50\%$. Final state interaction (FSI) calculations using the generalized Eikonal Approximation indicate that FSI should change the ^{3}He/^{3}H cross-section ratio for this measurement by less than 5%. If these calculations are correct, then the differences at large missing momenta between the ^{3}He/^{3}H experimental and calculated ratios could be due to the underlying NN interaction, and thus could provide new constraints on the previously loosely-constrained short-distance parts of the NN interaction.

Nuclear interaction models are a crucial starting point for modern calculations of nuclear structure and reactions, as well as the properties of dense astrophysical objects such as neutron stars. Phenomenological or meson-theoretic two-body potentials, such as Argonne-V18 (AV18) and CD-Bonn, were developed in the 1990s using constraints primarily from nucleon-nucleon (NN) scattering data [1,2]. More recently, chiral effective field theory (EFT) has led to the development of potentials with systematic and controlled approximations [3,4]. Light atomic nuclei have played a crucial role in constraining modern nuclear interaction models, including many-body forces, as many of their properties (e.g., charge distributions and radii, ground- and excited-state energies) can be both precisely measured and exactly calculated for a given two- and three-nucleon interaction model [5–10].

While the combination of NN scattering and light-nuclei data allows one to constrain the two- and three-nucleon interaction at large distances, its short-ranged behavior is still largely unconstrained. The latter is important for understanding nucleon-nucleon short-range correlations (SRC) in nuclei [11,12], their relation to the partonic structure of bound nucleons [13–17], and the structure of neutron stars [18,19].

Constraining the short-ranged part of the nuclear interaction requires studying nucleon momentum distributions at high-momentum. However, previous attempts to extract these were largely unsuccessful, due to the fact that nucleon momentum distributions are not direct observables, and typical experimental extractions suffer from large reaction mechanism effects. These introduce significant model-dependent corrections that mask the underlying characteristics of the momentum distribution, especially at high-momentum [20–23].

Advances in nuclear reaction theory now allow us to identify observables with increased sensitivity to nucleon momentum densities at high-momentum [18,24–27]. In light of these advances, we report on a new study of the momentum distribution of nucleons in Helium-3 relative to Tritium over a broad momentum range.

We study nucleon momentum distributions using Quasi-Elastic (QE) electron scattering. In these experiments, an electron with momentum $\vec{p}_e$ is scattered from the nucleus, transferring energy ω and momentum $\vec{q}$ to the nucleus. We choose ω and $\vec{q}$ to be appropriate for elastic scattering from a moving bound nucleon. By detecting the knocked-out proton ($\vec{p}_p$) in coincidence with the

scattered electron ($\vec{p}'_e$), we can measure the missing energy and missing momentum of the reaction:

$$E_{miss} = \omega - T_p - T_{A-1}, \quad (1)$$

$$\vec{p}_{miss} = \vec{p}_p - \vec{q}, \quad (2)$$

where $\vec{q} = \vec{p}_e - \vec{p}'_e$ is the momentum transfer, $T_{A-1} = (\omega + m_A - E_p) - \sqrt{(\omega + m_A - E_p)^2 - |\vec{p}_{miss}|^2}$ is the reconstructed kinetic energy of the residual $A-1$ system, and T_p and E_p are the measured kinetic and total energies of the outgoing proton.

In the Plane-Wave Impulse Approximation (PWIA) for QE scattering, where a single exchanged photon is absorbed on a single proton and the knocked-out proton does not re-interact as it leaves the nucleus, the cross-section for $A(e,e'p)$, electron-induced proton knockout from nucleus A, can be written as [28,29]:

$$\frac{d^6\sigma}{d\omega dE_p d\Omega_e d\Omega_p} = K\sigma_{ep} S(|\vec{p}_i|, E_i) \quad (3)$$

where σ_{ep} is the cross-section for scattering an electron from a bound proton [29], $K = E_p|\vec{p}_p|$ is a kinematical factor, $d\Omega_e$ and $d\Omega_p$ are the electron and proton solid angles respectively, and $S(|\vec{p}_i|, E_i)$ is the spectral function, which defines the probability to find a proton in the nucleus with momentum $|\vec{p}_i|$ and separation energy E_i. The nucleon momentum distribution is the integral of the spectral function over the separation energy: $n(|\vec{p}_i|) = \int S(|\vec{p}_i|, E_i) dE_i$.

In PWIA, the missing momentum and energy equal the initial momentum and separation energy of the knocked-out nucleon: $\vec{p}_i = \vec{p}_{miss}$, $E_i = E_{miss}$. However, there are other, non-QE, reaction mechanisms, including final state interactions (the rescattering of the knocked-out proton, FSI), meson-exchange currents (MEC), and exciting isobar configurations (IC) that can lead to the same measured final state. These also contribute to the cross section, complicating this simple picture. In addition, relativistic effects can be significant [30–32].

Previous measurements of the ^{3}He$(e,e'p)$ two- and three-body breakup cross-sections were done at $Q^2 = 1.5$ (GeV/c)^2 and $x_B \equiv \frac{Q^2}{2m_p\omega} = 1$ where m_p is the proton mass [21,22], near the expected maximum of the proton rescattering. The measured cross-sections disagreed by up to a factor of five with PWIA calculations for $p_{miss} > 250$ MeV/c. These deviations were described to good accuracy by calculations which included the contribution of non-QE reaction mechanisms, primarily FSI [18,24–26]. The large contribution of such non-QE reaction mechanisms to the measured $(e,e'p)$ cross-sections limited their ability to constrain the nucleon momentum distribution at high momenta.

Guided by reaction mechanism calculations, which agree with previous measurements, we can reduce the effect of FSI in two ways [25,27,33–37] by: (A) constraining the angle between $\vec{p}_{recoil} = -\vec{p}_{miss}$ and $\vec{q}$ to be $\theta_{rq} \lesssim 40^\circ$ and (B) taking the ratio of $(e,e'p)$ cross-sections for same-mass nuclei. The effect of FSI should be similar in both nuclei because knocked-out protons in both nuclei can rescatter from the same number of nucleons and FSI should therefore largely cancel in the ratio.

Additional non-QE reaction mechanisms such as MEC and IC were shown to be suppressed for $Q^2 \equiv q^2 - \omega^2 > 1.5$ (GeV/c)^2 and $x_B > 1$ [33,38]. Thus, the ratio of ^{3}He$(e,e'p)$ to ^{3}H$(e,e'p)$ cross-sections in QE kinematics at $Q^2 > 1.5$ (GeV/c)^2, $x_B > 1$ and $\theta_{rq} \lesssim 40^\circ$ should have increased sensitivity to the ratio of their spectral functions.

We measured the ratios of d, ^{3}He, and ^{3}H $(e,e'p)$ cross-sections in Hall A of the Thomas Jefferson National Accelerator Facility (JLab) using the two high-resolution spectrometers (HRS) and a 20 μA 4.326 GeV electron beam incident on one of four 25-cm long gas target cells [39]. The four identical cells were filled with Hydrogen (70.8 ± 0.4 mg/cm^2), Deuterium (142.2 ± 0.8 mg/cm^2), ^{3}He (53.4 ± 0.6 mg/cm^2) and Tritium (85.1 ± 0.8 mg/cm^2) gas [40]. We detected the scattered electrons in the left HRS at a central angle $\theta_e = 20.88^\circ$ and momentum $p_e = 3.543$ GeV/c, corresponding to a central four-momentum transfer $Q^2 = 2.0$ (GeV/c)^2, energy transfer $\omega = 0.78$ GeV, and $x_B = 1.4$. We detected the knocked-out protons in the right HRS at two different kinematical settings, (θ_p, p_p) = (48.82°, 1.481 GeV/c), and (58.50°, 1.246 GeV/c), referred to here as "low p_{miss}" and "high p_{miss}" respectively. These two settings cover a combined missing momentum range of $40 \leq p_{miss} \leq 550$ MeV/c. Deuterium measurements were only done in the "low p_{miss}" kinematics and thus extended only up to $p_{miss} \sim 300$ MeV/c.

Each HRS consisted of three quadrupole magnets for focusing and one dipole magnet for momentum analysis [43,44]. These magnets were followed by a detector package, slightly updated with respect to the one in Ref. [43], consisting of a pair of vertical drift chambers used for tracking, and two scintillation counter planes that provide timing and trigger signals. A CO_2 Cherenkov detector placed between the scintillators and a lead-glass calorimeter placed after them were used for particle identification.

Electrons were selected by requiring that the particle deposits more than half of its energy in the calorimeter: $\frac{E_{cal}}{|\vec{p}|} > 0.5$. $(e,e'p)$ coincidence events were selected by placing a $\pm 3\sigma$ cut around the relative electron and proton event times. Due to the low experimental luminosity, the random coincidence event rate was negligible. We discarded a small number of runs with anomalous numbers of events normalized to the beam charge.

Measured electrons were required to originate within the central ±9 cm of the gas target to exclude events originating from the target walls. The electron and proton reconstructed target vertices were required to be within ±1.2 cm of each other, which corresponds to $\pm 3\sigma$ of the vertex reconstruction resolution. By measuring scattering from an empty-cell-like target we determined that the target cell wall contribution to the measured $(e,e'p)$ event yield was negligible ($\ll 1\%$).

To avoid the acceptance edges of the spectrometer, we restricted the analysis to events that are detected within ±4% of the central spectrometer momentum, and ±27.5 mrad in in-plane angle and ±55.0 mrad in out-of-plane angle relative to the center of the spectrometer acceptance. In addition, we further restricted the measurement phase-space by requiring $\theta_{rq} < 37.5^\circ$ to minimize the effect of FSI and, in the high p_{miss} kinematics, $x_B > 1.3$ to further suppress non-QE events.

The spectrometers were calibrated using sieve slit measurements to define scattering angles and by measuring the kinematically over-constrained exclusive H$(e,e'p)$ and ^{2}H$(e,e'p)n$ reactions. The H$(e,e'p)$ reaction p_{miss} resolution was better than 9 MeV/c. We verified the absolute luminosity normalization by comparing the measured elastic H(e,e') yield to a parametrization of the world data [45]. We also found excellent agreement between the elastic H$(e,e'p)$ and H(e,e') rates, confirming that the coincidence trigger performed efficiently.

Fig. 1 shows the number of measured ^{3}H$(e,e'p)$ events as a function of E_{miss} and of Q^2 for the low p_{miss} setting as well as the same distributions calculated using the Monte Carlo code SIMC [41] and normalized to give the same integrated number of events as the data. SIMC generated $(e,e'p)$ events using Eq. (3), with the addition of radiation effects, that were then propagated through the spectrometer model to account for acceptance and resolution effects, and subsequently analyzed as the data. The SIMC calculations used a ^{3}He spectral function calculated by C. Ciofi degli Atti

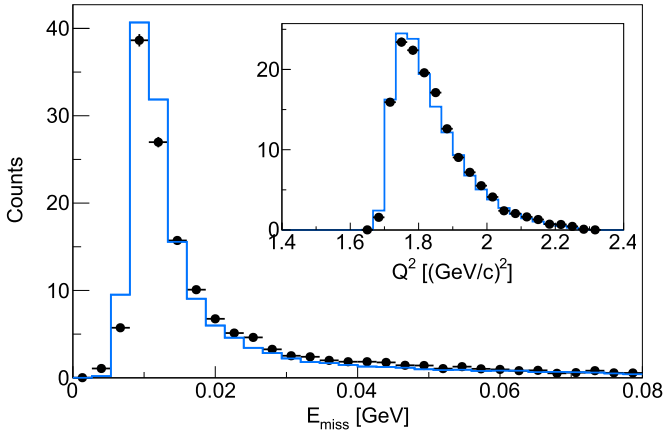

Fig. 1. Number of ^{3}H$(e,e'p)$ events (counts) versus missing energy for the low p_{miss} kinematics. The black markers correspond to the measured data. The lines correspond to the calculated distributions obtained from a SIMC [41] simulation with a spectral function calculated by C. Ciofi degli Atti and L. P. Kaptari [42] and normalized to give the same integral as the data. Due to the lack of ^{3}H proton spectral functions, we assumed isospin symmetry and used the ^{3}He neutron spectral function for the ^{3}H$(e,e'p)$ simulation (see text for details). The insert shows the Q^2 distribution for the same kinematical setting. See online supplementary materials for equivalent ^{3}He distributions.

and L. P. Kaptari using the AV18 potential [42]. Due to the lack of ^{3}H proton spectral functions, we assumed isospin symmetry and used the ^{3}He neutron spectral function for the ^{3}H$(e,e'p)$ simulation. The difference between the calculated momentum distributions of neutrons in ^{3}He and protons in ^{3}H is small and contributes a 3% uncertainty to the ^{3}H$(e,e'p)$ calculations and to the spectral-function ratio calculations [46]. The spectral function calculation appears to describe the measured Q^2 and E_{miss} distributions well. See online supplementary materials for details and additional comparisons (including ^{3}He$(e,e'p)$ spectra).

For each measured nucleus, we calculated the normalized $(e,e'p)$ event yield as:

$$Y(p_{miss}) = \frac{N(p_{miss})}{C \cdot t_{\rm live} \cdot (\rho/A) \cdot b}, \tag{4}$$

where A is the target atomic weight, $N(p_{miss})$ is the number of counts for that target in a given bin of p_{miss} integrated over the experimental E_{miss} acceptance, C is the total accumulated beam charge, $t_{\rm live}$ is the live time fraction in which the detectors are able to collect data, ρ is the nominal areal density of the gas in the target cell, and b is a correction factor to account for changes in the target density caused by local beam heating. b was determined by measuring the beam current dependence of the inclusive event yield [40]. We formed three yield ratios, ^{3}He/d, ^{3}H/d, and ^{3}He/^{3}H.

We corrected the measured ratio of the normalized yields for the radioactive decay of 2.78 ± 0.18% of the target ^{3}H nuclei to ^{3}He in the six months since the target was filled, and denote the corrected yield ratio by $R^{corr.yield}$.

The point-to-point systematical uncertainties on this ratio due to the event selection criteria (momentum and angular acceptances, and θ_{rq} and x_B limits) were determined by repeating the analysis 5000 times, selecting each criterion randomly within reasonable limits for each iteration. The systematic uncertainty was taken to be the standard deviation of the resulting distribution of ratios. They range from 1% to 8% and are typically much smaller than the statistical uncertainties. There is an overall normalization uncertainty of 1.8%, predominantly due to the target density uncertainty. Other normalization uncertainties due to beam-charge measurement and run-by-run stability are at the 1% level or lower, see Table 1. See online supplementary materials for details.

Table 1
Systematic uncertainties in the extraction of the ^{3}He/d, ^{3}H/d, and ^{3}He/^{3}H $(e,e'p)$ normalized event-yield ratios, $R^{corr.yield}_{^3\mathrm{He}/^3\mathrm{H}}$, (Fig. 2) and the ^{3}He/^{3}H cross-section ratio, $\sigma_{^3\mathrm{He}(e,e'p)}/\sigma_{^3\mathrm{H}(e,e'p)}$, (Fig. 3). Uncertainties marked by '*' contribute only to the cross-section ratio. All uncertainties are summed in quadrature. See text for details.

	Overall	Point-to-point
Target walls	$\ll 1$%	
Target density	1.5%	
Beam-charge and stability	1%	
Tritium decay	0.18%	
Cut sensitivity		1% - 8%
Simulation corrections* (bin-migration, radiation, E_m acceptance)		1% - 2%

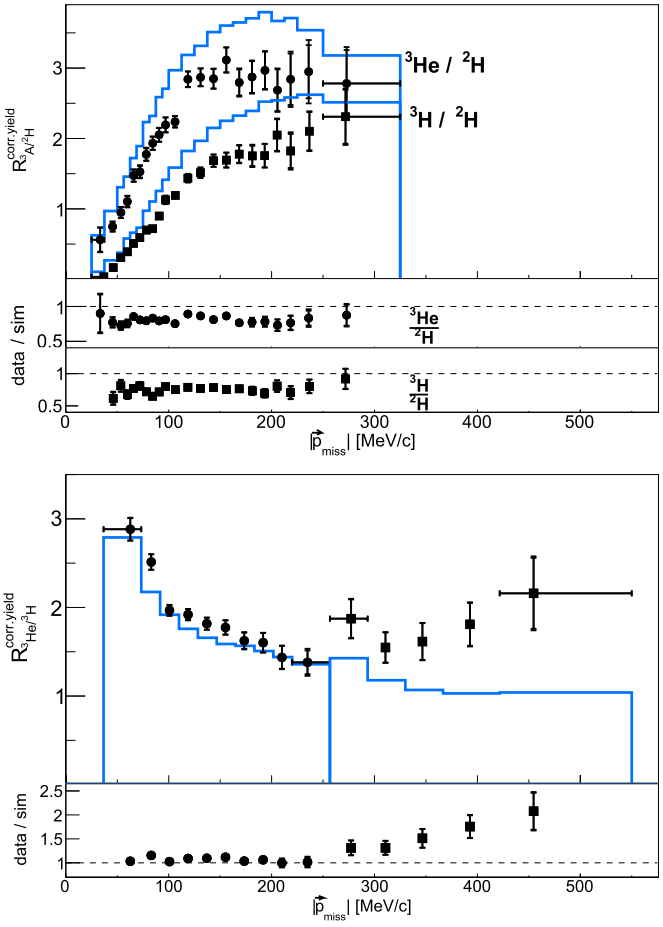

Fig. 2. Missing momentum dependence of the measured $(e,e'p)$ ^{3}He/d and ^{3}H/d (top) and ^{3}He/^{3}H (bottom) normalized event yield ratios. The circles and squares correspond respectively to ^{3}He/d and ^{3}H/d in the top panel and to the low and high p_{miss} settings in the bottom panel. The error bars include both statistical and point-to-point systematical uncertainties. An additional overall normalization uncertainty of 1.8% is not shown (see Table 1). The solid histogram shows the PWIA SIMC simulation using Eq. (3) and the spectral function of Ref. [42] for $A = 3$ and AV18 for $A = 2$. The bin widths are the same for the histogram and the data.

Fig. 2 shows the missing momentum dependence of the corrected event yield ratios $R^{corr.yield}_{^3\mathrm{He}/d}$, $R^{corr.yield}_{^3\mathrm{H}/d}$, and $R^{corr.yield}_{^3\mathrm{He}/^3\mathrm{H}}$ for each kinematical setting. The ratios of ^{3}He and ^{3}H to deuterium are very small at low p_{miss}, due to the much narrower deuterium momentum distribution, and increase to a constant value of about two for ^{3}H/d and about three for ^{3}He/d at the largest measured

p_{miss} of about 270 MeV/c. By contrast, the ^{3}He/^{3}H ratio is about three at the smallest measured p_{miss} and decreases to about 1.5 at $p_{miss} \approx 250$ MeV/c, with a possible rise after that. This is consistent with the low-p_{miss} expectation of 2.5 to 3 and slightly higher than the SRC-based high-p_{miss} expectation of one. The change in the ratios is much smaller than the four order-of-magnitude decrease in the calculated momentum distributions (see online supplementary information).

Both measured ^{3}He/d and ^{3}H/d ratios are about 20% larger than the PWIA spectral-function based SIMC calculation. This indicates that FSI effects are the same for both ratios. For the same missing momentum range, the measured and calculated ^{3}He/^{3}H ratios agree within the measurement accuracy of about 3%. This is a clear indication for cancellation of FSI effect in the ^{3}He/^{3}H ratio. At higher missing-momentum ($p_{miss} > 250$ MeV/c), the measured ^{3}He/^{3}H ratios are about $20-50$% larger than the calculation.

To extract the experimental cross-section ratio, $\sigma_{^3\mathrm{He}(e,e'p)}/\sigma_{^3\mathrm{H}(e,e'p)}(p_{miss})$, we corrected the measured yield ratios using SIMC for radiative and bin-migration effects as well as for the finite E_{miss} acceptance of the spectrometers. The finite E_{miss} correction equals the calculated momentum distribution ratio divided by the calculated ratio of spectral functions integrated over the missing energy acceptance. The individual and total corrections were all less than 10% for all p_{miss} values. We apply a point-to-point systematic uncertainty of 20% of the resulting correction factors. See Table 1 and online supplementary material for details.

We also calculated the final state interaction effects of single rescattering of the knocked-out proton with either of the two other nucleons in the three-body-breakup reaction in the generalized Eikonal approximation [47,48] using a computer code developed by M. Sargsian [49]. For each bin we calculated both the PWIA and FSI cross section and integrated over the experimental acceptance. FSI changed the individual ^{3}He and ^{3}H$(e,e'p)$ cross-sections by between 10% and 30%. However, they largely cancelled in the double ratio

$$R^{FSI} = \frac{\sigma_{FSI}/\sigma_{PWIA}|_{^3\mathrm{He}}}{\sigma_{FSI}/\sigma_{PWIA}|_{^3\mathrm{H}}}, \quad (5)$$

producing at most a 5% effect at the highest p_{miss}. This reinforces the claim that FSI effects are very small in the cross-section ratio. We did not correct the data for FSI. See online supplementary materials for more information.

We tested the cross section factorization approximation by comparing the factorized spectral function approach used in SIMC with an unfactorized calculation by J. Golak [50–52]. The difference between the factorized and non-factorized calculations was about 5%, which is not enough to explain the data-calculation discrepancy at high p_{miss}.

Fig. 3 shows the p_{miss} dependence of the extracted ^{3}He/^{3}H $(e,e'p)$ cross-section ratio. In the simplest model, this ratio should equal two, the relative number of protons in ^{3}He and ^{3}H. However, at large p_{miss} the ratio should equal one, the relative number of np SRC pairs in ^{3}He and ^{3}H [53–61]. These SRC pairs will shift equal amounts of cross-section strength from low p_{miss} to high p_{miss} in both nuclei, increasing the ^{3}He to ^{3}H ratio at low p_{miss} to more than two. The measured ratio follows this simple model of a transition from independent nucleons at the lowest p_{miss} to np-SRC pairs at higher p_{miss}, decreasing from almost three at low p_{miss} towards about 1.5 at $p_{miss} = 250$ MeV/c. At larger p_{miss} the measured ratio is approximately flat, with a possible rise at the largest p_{miss}.

With the missing-energy acceptance correction for ^{3}He/^{3}H and the small expected FSI effects, the resulting cross-section ratios should be sensitive to the ratio of momentum distributions. We

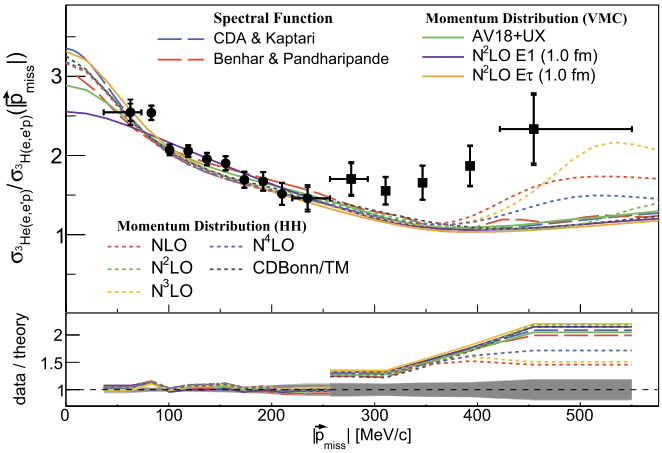

Fig. 3. The measured ^{3}He to ^{3}H cross-section ratio, $\sigma_{^3\mathrm{He}(e,e'p)}/\sigma_{^3\mathrm{H}(e,e'p)}(p_{miss})$, plotted vs. p_{miss} compared with different models of the corresponding momentum distribution ratio. The filled circle and square markers correspond to the low and high p_{miss} settings respectively. Uncertainties shown include both statistical and point-to-point systematical uncertainties. The overall normalization uncertainty of about 1.8% is not shown (see Table 1). Horizontal bars indicate the bin sizes and are shown for only the first and last points in each kinematical setting as all other points are equally spaced. The bottom panel shows the double ratio of data to different calculated momentum distribution ratios, with the grey band showing the data uncertainty. The theoretical calculations are done using different local and non-local interactions, as well as different techniques for solving the three-body problem. See text for details.

therefore compare in Fig. 3 the measured cross-section ratios directly with the ratio of various single-nucleon momentum distributions. The momentum distribution calculations are obtained using either the variational Monte Carlo (VMC) technique with local interactions [46,62] or the Hyperspherical Harmonics (HH) method [63,64] with non-local interactions.

The local interactions used include the phenomenological AV18 [2] two-nucleon potential augmented by the Urbana X (UX) [65] three-nucleon force and the chiral EFT potentials at N^{2}LO (including two- and three-body contributions), using a coordinate-space cutoff of 1 fm and different parametrizations of the three-body contact term $E\tau$ and $E1$ [10,66–69]. Non-local interactions include the meson-theoretic CD-Bonn [70] two-nucleon potential, together with the Tucson-Melbourne [71] (TM) three-nucleon potential, or the latest chiral two-body potentials from NLO to N^{4}LO [72], including three-nucleon interactions. The main contribution to the latter, namely the one arising from two-pion exchange, is effectively included at the same chiral order as the two-nucleon interaction, as explained in Refs. [64,72]. In these calculations, the momentum-space cutoff Λ is kept fixed at 500 MeV. The VMC calculations using the AV18 and UX interactions produce equivalent results as the HH calculations using the AV18 plus Urbana IX [73] interactions.

For completeness, Fig. 3 also shows the momentum-distribution ratio calculated by integrating over the missing energy in the spectral functions of Ref. [42] and Ref. [74], obtained using the AV18 two-nucleon only and the AV14 [75] two- and the Urbana VIII [76] (UVIII) three-nucleon interactions, respectively.

All calculated momentum-distribution ratios shown agree with the data up to $p_{miss} \approx 250$ MeV/c. At larger p_{miss}, the theoretical predictions obtained by integrating the spectral functions or by calculating the momentum distribution ratio with local potentials or with the CD-Bonn/TM model disagree with the data by 20–50%. In the case of the non-local chiral potential models, the calculations show significant order dependence.

Note that, while momentum distributions calculated with local chiral-interactions depend strongly on the cutoff parameter, these

effects appear to mostly cancel in the ratio of the momentum distributions [77].

Finally, although FSI calculated in the generalized Eikonal approximation are small, more complete calculations are needed, including two- and three-body interaction operators [78], to determine if the discrepancy between data and calculation is due to the reaction mechanism or to the validity of the underlying NN potentials at short-distances. In addition, fully relativistic calculations are needed to see if there are any significant corrections due to longitudinal-transverse interference effects [30–32].

One possible explanation for the discrepancy could be single-charge exchange FSI, where a struck neutron from an SRC rescatters at almost 180° from a proton, and the proton is detected (np SCX), or a struck proton from an SRC rescatters at almost 180° from a neutron (pn SCX). A struck proton in an SRC rescattering from its partner neutron will decrease the number of observed proton events and a struck neutron in an SRC rescattering from its partner proton will increase the number of observed proton events. These two effects will largely cancel in both ^{3}He$(e,e'p)$ and ^{3}H$(e,e'p)$. However, in ^{3}He the struck neutron in an SRC can rescatter from the uncorrelated proton, increasing the number of observed proton events but in ^{3}H it cannot. This can increase the observed ^{3}He/^{3}H ratio. In addition, if the SCX occurs at $\theta < 180°$, then events at small p_{miss} will be observed at larger p_{miss}, amplifying the effects of SCX at large p_{miss}.

To summarize, we presented the first simultaneous measurement of the ^{3}He$(e,e'p)$, ^{3}H$(e,e'p)$ and $d(e,e'p)$ reactions in kinematics where the cross-sections are expected to be sensitive to the proton momentum distribution, i.e., at large Q^2, $x_B > 1$, and $\theta_{rq} < 40°$ that minimize two-body currents and the effects of FSI. We further enhanced the sensitivity to the momentum distribution by extracting the ratio of the cross-sections, so that most of the remaining FSI effects cancel, as confirmed by a generalized Eikonal approximation calculation of leading proton rescattering.

The measured ^{3}He/d and ^{3}H/d corrected yield ratios are small at low p_{miss} and increase to three and two respectively at $p_{miss} =$ 250 MeV/c. Both are about 20% lower than PWIA calculated yield ratios, indicating that FSI effects are about the same in both pairs of reactions.

While the measured corrected cross-section ratio $\sigma_{^3\mathrm{He}(e,e'p)}/\sigma_{^3\mathrm{H}(e,e'p)}$ is well described by PWIA calculations up to $p_{miss} \approx 250$ MeV/c, they disagree by only 20 - 50% at high p_{miss}, despite a four order of magnitude decrease of the momentum distribution in this range (see Fig. 2 of the online supplementary information). This is a vast improvement over previous $\sigma_{^3\mathrm{He}(e,e'p)}$ measurements at lower Q^2 and $x_B = 1$, which disagreed with PWIA calculations by factors of several at large p_{miss} [21,22]. This, together with FSI calculations, strongly supports the reduced contribution of non-QE reaction mechanisms in our kinematics.

The data overall supports the transition from single-nucleon dominance at low p_{miss}, towards an np-SRC pair dominant region at high p_{miss} [53–61]. However, more complete calculations are needed to assess the implications of the observed 20–50% deviation of the data from the PWIA calculation in the expected np-SRC pair dominance region, including the effects of single charge exchange. If the observed difference between the ^{3}He/^{3}H experimental ratio and momentum distribution ratios at large missing momenta is due to the underlying NN interaction, then it can provide significant new constraints on the previously loosely-constrained short-distance parts of the NN interaction.

Acknowledgements

We acknowledge the contribution of the Jefferson-Lab target group and technical staff for design and construction of the Tritium target and their support running this experiment. We thank C. Ciofi degli Atti and L. Kaptari for the ^{3}He spectral function calculations and M. Sargsian, M. Strikman, J. Carlson, S. Gandolfi, and R. B. Wiringa for many valuable discussions. This work was supported by the U.S. Department of Energy (DOE) grant DE-AC05-06OR23177 under which Jefferson Science Associates, LLC, operates the Thomas Jefferson National Accelerator Facility, the U.S. National Science Foundation, the Pazi foundation, the Israel Science Foundation, and the NUCLEI SciDAC program. Computational resources for the calculation of the N^{2}LO momentum distributions have been provided by Los Alamos Open Supercomputing via the Institutional Computing (IC) program and by the National Energy Research Scientific Computing Center (NERSC), which is supported by the U.S. Department of Energy, Office of Science, under Contract No. DE-AC02-05CH11231. The Kent State University contribution is supported under the PHY-1714809 grant from the U.S. National Science Foundation. The University of Tennessee contribution is supported by the DE-SC0013615 grant. The work of ANL group members is supported by DOE grant DE-AC02-06CH11357.

Appendix A. Supplementary material

Supplementary material related to this article can be found online at https://doi.org/10.1016/j.physletb.2019.134890.

References

[1] R. Machleidt, K. Holinde, C. Elster, Phys. Rep. 149 (1987) 1.
[2] R.B. Wiringa, V.G.J. Stoks, R. Schiavilla, Phys. Rev. C 51 (1995) 38, arXiv:nucl-th/9408016 [nucl-th].
[3] R. Machleidt, D.R. Entem, Phys. Rep. 503 (2011) 1.
[4] E. Epelbaum, H.-W. Hammer, U.-G. Meissner, Rev. Mod. Phys. 81 (2009) 1773, arXiv:0811.1338 [nucl-th].
[5] J. Carlson, R. Schiavilla, Rev. Mod. Phys. 70 (1998) 743.
[6] J. Carlson, S. Gandolfi, F. Pederiva, S.C. Pieper, R. Schiavilla, K.E. Schmidt, R.B. Wiringa, Rev. Mod. Phys. 87 (2015) 1067, arXiv:1412.3081 [nucl-th].
[7] M. Piarulli, L. Girlanda, R. Schiavilla, A. Kievsky, A. Lovato, L.E. Marcucci, S.C. Pieper, M. Viviani, R.B. Wiringa, Phys. Rev. C 94 (2016) 054007.
[8] G. Hagen, T. Papenbrock, M. Hjorth-Jensen, D.J. Dean, Rep. Prog. Phys. 77 (2014) 096302.
[9] B.R. Barrett, P. Navrátil, J.P. Vary, Prog. Part. Nucl. Phys. 69 (2013) 131.
[10] D. Lonardoni, S. Gandolfi, J.E. Lynn, C. Petrie, J. Carlson, K.E. Schmidt, A. Schwenk, Phys. Rev. C 97 (2018) 044318.
[11] O. Hen, G.A. Miller, E. Piasetzky, L.B. Weinstein, Rev. Mod. Phys. 89 (2017) 045002, arXiv:1611.09748 [nucl-ex].
[12] C. Ciofi degli Atti, Phys. Rep. 590 (2015) 1.
[13] B. Schmookler, M. Duer, A. Schmidt, et al., CLAS, Nature 566 (2019) 354.
[14] J.-W. Chen, W. Detmold, J.E. Lynn, A. Schwenk, Phys. Rev. Lett. 119 (2017) 262502, arXiv:1607.03065 [hep-ph].
[15] L.B. Weinstein, E. Piasetzky, D.W. Higinbotham, J. Gomez, O. Hen, R. Shneor, Phys. Rev. Lett. 106 (2011) 052301, arXiv:1009.5666 [hep-ph].
[16] O. Hen, E. Piasetzky, L.B. Weinstein, Phys. Rev. C 85 (2012) 047301, arXiv:1202.3452 [nucl-ex].
[17] O. Hen, D.W. Higinbotham, G.A. Miller, E. Piasetzky, L.B. Weinstein, Int. J. Mod. Phys. E 22 (2013) 1330017, arXiv:1304.2813 [nucl-th].
[18] L. Frankfurt, M. Sargsian, M. Strikman, Int. J. Mod. Phys. A 23 (2008) 2991, arXiv:0806.4412 [nucl-th].
[19] B.-A. Li, B.-J. Cai, L.-W. Chen, J. Xu, Prog. Part. Nucl. Phys. 99 (2018) 29, arXiv:1801.01213 [nucl-th].
[20] A. Bussiere, J. Mougey, D. Royer, D. Tarnowski, S. Turck-Chieze, M. Bernheim, S. Frullani, G.P. Capitani, E. De Sanctis, E. Jans, Nucl. Phys. A 365 (1981) 349.
[21] F. Benmokhtar, et al., Jefferson Lab Hall A, Phys. Rev. Lett. 94 (2005) 082305, arXiv:nucl-ex/0408015 [nucl-ex].
[22] M.M. Rvachev, et al., Jefferson Lab Hall A, Phys. Rev. Lett. 94 (2005) 192302, arXiv:nucl-ex/0409005 [nucl-ex].
[23] K.S. Egiyan, et al., CLAS, Phys. Rev. Lett. 98 (2007) 262502, arXiv:nucl-ex/0701013 [nucl-ex].
[24] C. Ciofi degli Atti, L.P. Kaptari, Phys. Rev. Lett. 95 (2005) 052502, arXiv:nucl-th/0502045 [nucl-th].
[25] J.M. Laget, Phys. Lett. B 609 (2005) 49, arXiv:nucl-th/0407072 [nucl-th].
[26] M. Alvioli, C. Ciofi degli Atti, L.P. Kaptari, Phys. Rev. C 81 (2010) 021001, arXiv:0904.4045 [nucl-th].
[27] W.U. Boeglin, et al., Hall A, Phys. Rev. Lett. 107 (2011) 262501, arXiv:1106.0275 [nucl-ex].

[28] J.J. Kelly, Adv. Nucl. Phys. 23 (1996) 75.
[29] T. De Forest, Nucl. Phys. A 392 (1983) 232.
[30] J. Gao, et al., The Jefferson Lab Hall A Collaboration, Phys. Rev. Lett. 84 (2000) 3265.
[31] J.M. Udias, J.A. Caballero, E. Moya de Guerra, J.E. Amaro, T.W. Donnelly, Phys. Rev. Lett. 83 (1999) 5451.
[32] R. Alvarez-Rodriguez, J.M. Udias, J.R. Vignote, E. Garrido, P. Sarriguren, E. Moya de Guerra, E. Pace, A. Kievsky, G. Salme, in: Proceedings, 21st European Conference on Few-Body Problems in Physics (EFB21), Salamanca, Castilla y Leon, Spain, August 29-September 3, 2010, Few-Body Syst. 50 (2011) 359, arXiv:1012.3049 [nucl-th].
[33] M.M. Sargsian, Int. J. Mod. Phys. E 10 (2001) 405, arXiv:nucl-th/0110053 [nucl-th].
[34] L.L. Frankfurt, M.M. Sargsian, M.I. Strikman, Phys. Rev. C 56 (1997) 1124, arXiv:nucl-th/9603018 [nucl-th].
[35] S. Jeschonnek, J.W. Van Orden, Phys. Rev. C 78 (2008) 014007, arXiv:0805.3115 [nucl-th].
[36] M.M. Sargsian, Phys. Rev. C 82 (2010) 014612, arXiv:0910.2016 [nucl-th].
[37] O. Hen, L.B. Weinstein, S. Gilad, W. Boeglin, Proton and neutron momentum distributions in A = 3 asymmetric nuclei, arXiv:1410.4451 [nucl-ex], 2014.
[38] M.M. Sargsian, et al., J. Phys. G 29 (2003) R1, arXiv:nucl-th/0210025 [nucl-th].
[39] D. Meekins, Jefferson Lab Engineering Report, 2017.
[40] S.N. Santiesteban, et al., arXiv:1811.12167 [physics.ins-det], 2018.
[41] SIMC, https://hallcweb.jlab.org/wiki/index.php/SIMC_Monte_Carlo. (Accessed 11 October 2018).
[42] C. Ciofi degli Atti, L.P. Kaptari, Phys. Rev. C 71 (2005) 024005, arXiv:nucl-th/0407024 [nucl-th].
[43] J. Alcorn, et al., Nucl. Instrum. Methods Phys. Res., Sect. A 522 (2004) 294.
[44] In 2016, the Quadrupole magnet closest to the target (Q1) was replaced with a normal conducting quad, with similar magnetic properties.
[45] E.L. Lomon, arXiv:nucl-th/0609020 [nucl-th], 2006.
[46] R.B. Wiringa, R. Schiavilla, S.C. Pieper, J. Carlson, Phys. Rev. C 89 (2014) 024305.
[47] M.M. Sargsian, T.V. Abrahamyan, M.I. Strikman, L.L. Frankfurt, Phys. Rev. C 71 (2005) 044614.
[48] M.M. Sargsian, T.V. Abrahamyan, M.I. Strikman, L.L. Frankfurt, Phys. Rev. C 71 (2005) 044615.
[49] M. Sargsian, Private communication.
[50] C. Carasco, et al., Phys. Lett. B 559 (2003) 41.
[51] J. Bermuth, et al., Phys. Lett. B 564 (2003) 199.
[52] J. Golak, R. Skibinski, H. Witala, W. Glockle, A. Nogga, H. Kamada, Phys. Rep. 415 (2005) 89, arXiv:nucl-th/0505072 [nucl-th].
[53] R. Weiss, R. Cruz-Torres, N. Barnea, E. Piasetzky, O. Hen, Phys. Lett. B 780 (2018) 211, arXiv:1612.00923 [nucl-th].
[54] E. Piasetzky, M. Sargsian, L. Frankfurt, M. Strikman, J.W. Watson, Phys. Rev. Lett. 97 (2006) 162504.
[55] A. Tang, et al., Phys. Rev. Lett. 90 (2003) 042301.
[56] R. Shneor, et al., Phys. Rev. Lett. 99 (2007) 072501.
[57] R. Subedi, et al., Science 320 (2008) 1476.
[58] I. Korover, N. Muangma, O. Hen, et al., Phys. Rev. Lett. 113 (2014) 022501.
[59] O. Hen, et al., Science 346 (2014) 614, arXiv:1412.0138 [nucl-ex].
[60] M. Duer, et al., CLAS, Nature 560 (2018) 617.
[61] M. Duer, et al., CLAS Collaboration, Phys. Rev. Lett. 122 (2019) 172502.
[62] D. Lonardoni, S. Gandolfi, X.B. Wang, J. Carlson, Phys. Rev. C 98 (2018) 014322.
[63] A. Kievsky, S. Rosati, M. Viviani, L.E. Marcucci, L. Girlanda, J. Phys. G 35 (2008) 063101, arXiv:0805.4688 [nucl-th].
[64] L.E. Marcucci, F. Sammarruca, M. Viviani, R. Machleidt, arXiv:1809.01849 [nucl-th], 2018.
[65] R.B. Wiringa, Single-nucleon momentum distributions, http://www.phy.anl.gov/theory/research/momenta, 2018, last update: August 6, 2018.
[66] A. Gezerlis, I. Tews, E. Epelbaum, M. Freunek, S. Gandolfi, K. Hebeler, A. Nogga, A. Schwenk, Phys. Rev. C 90 (2014) 054323.
[67] J.E. Lynn, I. Tews, J. Carlson, S. Gandolfi, A. Gezerlis, K.E. Schmidt, A. Schwenk, Phys. Rev. Lett. 116 (2016) 062501.
[68] J.E. Lynn, I. Tews, J. Carlson, S. Gandolfi, A. Gezerlis, K.E. Schmidt, A. Schwenk, Phys. Rev. C 96 (2017) 054007.
[69] D. Lonardoni, J. Carlson, S. Gandolfi, J.E. Lynn, K.E. Schmidt, A. Schwenk, X.B. Wang, Phys. Rev. Lett. 120 (2018) 122502.
[70] R. Machleidt, Phys. Rev. C 63 (2001) 024001, arXiv:nucl-th/0006014 [nucl-th].
[71] S.A. Coon, H.K. Han, Few-Body Syst. 30 (2001) 131, arXiv:nucl-th/0101003 [nucl-th].
[72] D.R. Entem, R. Machleidt, Y. Nosyk, Phys. Rev. C 96 (2017) 024004, arXiv:1703.05454 [nucl-th].
[73] B.S. Pudliner, V.R. Pandharipande, J. Carlson, R.B. Wiringa, Phys. Rev. Lett. 74 (1995) 4396, arXiv:nucl-th/9502031 [nucl-th].
[74] O. Benhar, V.R. Pandharipande, Phys. Rev. C 47 (1993) 2218.
[75] R.B. Wiringa, R.A. Smith, T.L. Ainsworth, Phys. Rev. C 29 (1984) 1207.
[76] J. Carlson, V.R. Pandharipande, R.B. Wiringa, Nucl. Phys. A 401 (1983) 59.
[77] D. Lonardoni, S. Gandolfi, X.B. Wang, J. Carlson, Phys. Rev. C 98 (2018) 014322, arXiv:1804.08027 [nucl-th].
[78] S.N. More, S.K. Bogner, R.J. Furnstahl, Phys. Rev. C 96 (2017) 054004.